

Kent Academic Repository

Full text document (pdf)

Citation for published version

Njogu, Peter, Izquierdo, Benito, Gao, Stephen and Chen, Zhijiao Disposable 3D printed Liquid sensor. In: EuCAP2022.

DOI

Link to record in KAR

<https://kar.kent.ac.uk/96093/>

Document Version

Author's Accepted Manuscript

Copyright & reuse

Content in the Kent Academic Repository is made available for research purposes. Unless otherwise stated all content is protected by copyright and in the absence of an open licence (eg Creative Commons), permissions for further reuse of content should be sought from the publisher, author or other copyright holder.

Versions of research

The version in the Kent Academic Repository may differ from the final published version.

Users are advised to check <http://kar.kent.ac.uk> for the status of the paper. **Users should always cite the published version of record.**

Enquiries

For any further enquiries regarding the licence status of this document, please contact:

researchsupport@kent.ac.uk

If you believe this document infringes copyright then please contact the KAR admin team with the take-down information provided at <http://kar.kent.ac.uk/contact.html>

Disposable 3D printed Liquid sensor

Peter Njogu¹, Benito Izquierdo¹, Stephen Gao¹ and Zhijiao Chen²

¹School of Engineering University of Kent, Canterbury, UK, pmn20@kent.ac.uk, b.sanz@kent.ac.uk

²School of Electronic Engineering, Beijing University of Posts and Telecommunications, Beijing, China

Abstract— A device for detecting liquid chemicals of various permittivity using a 3D Printed frequency selective surface (FSS) is proposed. The sensor is an array of square loops on a square unit cell with trenches dug in the dielectric material around the loops. The trenches allow deposition of the liquid chemicals to be detected. The variation in the dielectric characteristics of the liquids in the trenches produces a change in the resonance frequency of the FSS. Transmission coefficient is measured to evaluate the resonance frequency due to each liquid chemical. Butan-1-ol, Propan-2-ol, Ethanol and Methanol were added to demonstrate the sensing technique. Good agreement was found to exist between simulated and measured results. The envisioned detector could be used in a laboratory or in chemical industry where liquids can fall into the trenches for detection purpose. 3D printing allows for the rapid fabrication of the structure which can be disposable.

Index Terms—FSS, FFF, Sensor, periodic structure, Liquid chemicals.

I. INTRODUCTION

Industrial chemicals e.g., Methanol, Ethanol, Butanol etc. can be hazardous to health especially in unventilated closed spaces. Inhalation of such vapour can cause toxicity as well as skin and eye irritation [1] and [2]. Identification of chemicals without without being close to them would reduce hazard. This can be achieved through use of microwave sensors.

A number of microwave liquid sensing method have been devised and developed using different methods. A Chipless slotted cylindrical resonator liquid Sensor is presented in [3] while [4] presents a UHF RFID antenna based sensor for aqueous and organic liquids. A microwave biosensor that detects glucose level in aqueous solution is presented in [5] while [6] is a Terahertz biosensor integrated with microfluidics for Liver Cancer Biomarker. A real time microwave biochemical sensor based on circular substrate integrated waveguide (SIW) approach for aqueous dielectric detection is demonstrated in [7]

Metamaterials have also been investigated in liquid microwave sensing . A split ring resonator (SRR) based liquid sensor with fluidic capillary to hold the liquid to be tested is demonstrated in [8]. The concept of the SRR based sensing is advanced to Complementary Split Ring Resonator (CSRR) resonator sensor as demonstrated in [9] [10] [11] [12] [13] and [14].

Electromagnetic band gap (EBG) based have also recently been explored in wireless liquid sensing. A multilayer reconfigurable electromagnetic bandgap structure (EBG) based sensor/detector has recently been proposed as liquid detector application [15]. This work is advanced in [16] as a

Casero fractal based EBG microwave sensing platform. The above referenced liquid sensing platforms offers good measurement accuracy and sensitivity. However, they are complex in design and operation, bulk and others require delicate and intricate assembly. Extra costs accrue due to extra parts e.g., capillaries, capsules, and liquid containers. Other designs like EBG are multipart requiring intricate assembly beside their design complexity.

This work proposes a simple, inexpensive, easy to fabricate, use and assemble, compact single unit, FSS based sensor. An FSS is a periodic surface of identical conductors arranged in one or two-dimensional infinite array [17]. The dielectric layer of the FSS was fabricated using fused filament fabrication (FFF). FFF was employed because it enables the creation of detailed and intricate objects allowing engineers to test parts for fit and form [18]. In the fabrication process, trenches were made between the between square unit cell elements. These trenches were filled with liquids of different dielectric permittivity. The FSS conductive elements were painted onto the FFF printed substrate using silver ink. CST Microwave StudioTM has been employed in the design, simulation, and optimization of the sensor.

II. THE FSS SENSOR DEVELOPMENT

A. The sensor design and simulations

Square loops FSS [19] band stop array was employed in this work as it offers dual polarization and good angle of incidence behavior [20]. Square loop FSS resonates when the circumference of the loop is about a wavelength of the resonance frequency.

A 20 mm x 20 mm x 5.2 mm square unit cell was simulated on a Polylactic acid (PLA) substrate of relative permittivity of 2.4 and a $\tan \delta$ of 0.01 [21]. A 2 mm wide, 18 mm x 18 mm square loop simulated onto the unit cell. A 1 mm wide and 2 mm deep trench was dug around the unit cell edges by partially removing the substrate around the square loop. The geometry of the unit cell is shown in Fig. 1. The perspective view of unit cell is shown in Fig. 1 (a) while the front and cross-sectional views are shown in Fig. 1(b) and Fig. 1(d) respectively. The square loop was optimized to operate at a frequency of 4.4 GHz. Gap x between the conductor loop and the edge of the cell is 1 mm while the gap g between two adjacent square loops is 2 mm. The periodicity, P , of the square loop array is the sum of g and the length d_2 of the square loop i.e., 18 mm. d_1 represent the length of the unit cell. The main design parameters values of the unit cell are represented in Table 1.

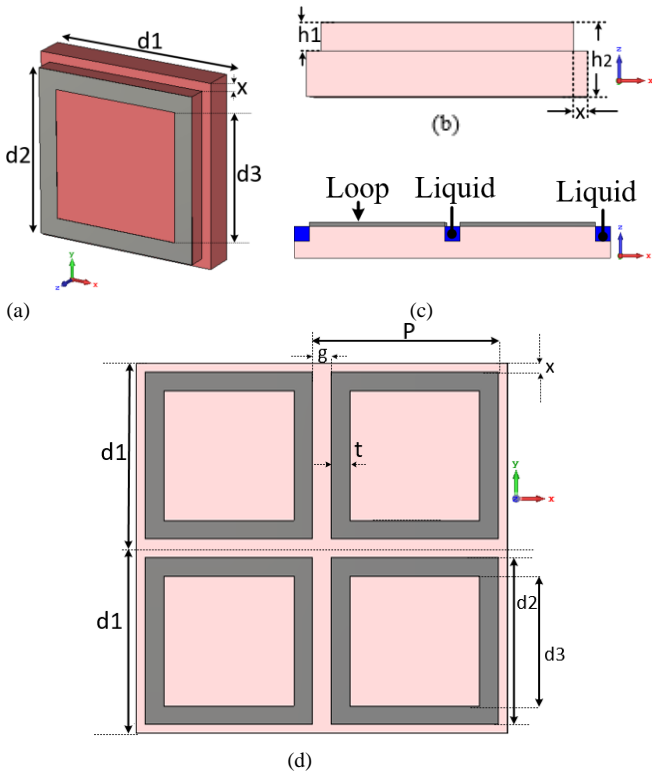


Fig. 1 shows (a) the perspective view (b) the cross-sectional view (c) cross sectional view of a section of the FSS sensor liquid-filled trenches (d) the top view of the unit cell

TABLE I
Dimensions of the unit cell

Dimensions	d1	d2	d3	h1	h2	P	g	t	x
Value (mm)	20	18	14	2	5.2	20	2	2	1

B. Simulation results of the sensor

The designed sensor was simulated to test its behavior in terms of transmission coefficient. Fig. 2 shows the simulated transmission response, S_{21} of the FSS for TE angle of incidence behaviors at 0° and 45° and TM angle of incidence at 45° measured in free space. TE denotes the E-plane response whereas TM denotes H-plane response. The results indicates that the resonance of the unit cell occurred at normal incidence with a frequency of 4.43 GHz with no appreciable frequency drift at TE 45° and TM 45° . The resonance frequency of the unit cell in air i.e., free space was considered the sensor's reference point.

Simulations were then conducted with the trenches filled with various liquids under test as shown in Fig. 1(c). The liquids that were tested were Butanol-1-o1, Propan-2-o1, Ethanol, and Methanol whose electrical characteristics at 5GHz and temperature of 20° are shown in Table II [22]. The simulation results are presented in Fig. 3 and Table III and shows that when a chemical dielectric fills the trenches behind the loop, the band stop center frequency shifts to the left. This indicates that stopband of the FSS can be tuned using the liquid dielectrics. The results shows that the liquids with higher ϵ_r , produces a bigger frequency shift, Δf , from the reference

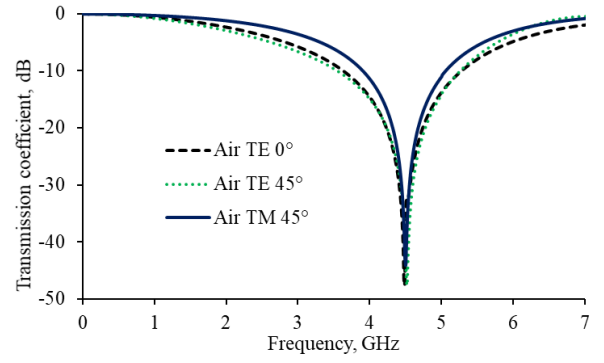


Fig. 2 Simulated transmission responses of the loop FSS

TABLE II
ELECTRICAL CHARACTERISTICS OF UNDER-TEST CHEMICALS

Liquid	Relative permittivity ϵ_r	Loss tangent ($\tan \delta$)
Butan-1-o1	3.29	0.47
Propan-2-o1	3.8	0.64
Ethanol	5.08	0.96
Methanol	12.42	0.65

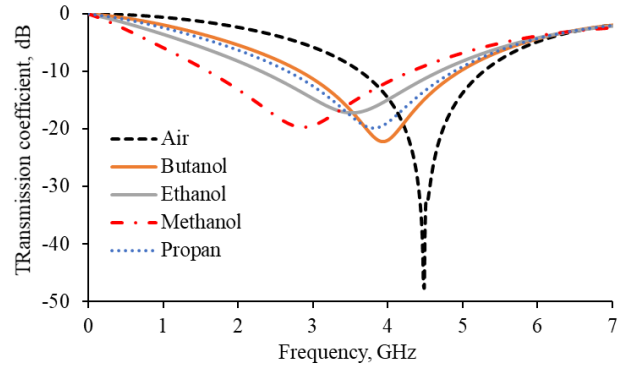


Fig. 3 The simulated frequency response of the proposed sensor structure for the various liquid chemicals

TABLE III
SIMULATED RESONANCE FREQUENCY AND SHIFT FROM REFERENCE FREQUENCY

	Butanol-1-o1	Ethanol	Methanol	Propan-2-o1
f_s GHz	3.92	3.50	2.87	3.80
Δf GHz	0.51	0.93	1.56	0.63

frequency i.e. the resonance frequency, 4.43 GHz, when the trenches are air-filled which is commensurate with [23]. It is also observed that the results due to Butanol-1-o1 and Propan-2-o1 are nearly indistinguishable. This is due to their close dielectric constant values. This indicate that effectiveness of the sensor depend on the amount of separation between the dielectric constants of the two chemical liquids.

III. FABRICATION AND MEASUREMENT

A. Fabrication

The sensor fabrication was a two-stage process. The first stage was the printing of polylactide acid (PLA) substrate material. To begin the process, the simulated design unit cell was first extended to a 9×9 array to create a model of the

proposed sensor. An outer 5 mm wide perimeter edge, 1 mm higher, for liquid containment, was incorporated, making it a 192 mm x 192 mm structure. The cell edges were also raised by 0.175 mm in order to facilitate application of the silver conductive paint without it flowing onto the surface of the unit cells.

To start the fabrication process, the digital model of the FSS substrate was exported from CST Microwave Studio to an STL file. It was then sent to a Raised 3D printer machine shown in Fig. 4(a), using CURA software with the print infill density of the print set to 100% which printed the structure as a 26 layers FFF printout. The FFF printed structure substrate material is shown in Fig. 4(b).

The second stage involved the application of the RS pro Silver Conductive 186-3600 paint [24], Fig. 4(c), onto the substrate to create the conductive loops. The conductive loops were by-hand painted around the cells on the substrate using an artist's painting brush. To ensure that this was done in the best way possible and that the width of the loop's conductor was maintained uniformly, a stencil was printed and employed in the application of the paint. This shown in Fig. 4(d). The stencil was printed alongside the substrate. The FFF printed substrate with the manually by-hand painted square loops is shown in Fig. 4(e). The manually applied silver paint was left for 24 hours to dry. Fig. 4(f) shows the finished

B. Measurements and results

Using a Marconi Instruments microwave test set 6204B in a plain wave chamber, the transmission coefficient S_{21} of the FSS was measured with empty trenches. Fig 4(g) shows the measurements set up. The trenches were then filled with the liquid chemicals and S_{21} measured to obtain the resonance points of each liquid chemical. The measured frequency resonance of the liquid chemicals deposited in the trenches of the FFF printed FSS sensor were found to be as shown in Fig. 5. Table IV shows the measured resonance frequency, f_s , and the frequency shift, Δf , from the reference. The results show a trend in frequency shift from the reference frequency i.e. air resonance frequency, consistent with the simulation results. The resonance frequency progressively shifts to lower frequencies as liquid chemicals with higher dielectric constant is deposited in the trenches.

It was observed that the resonance frequency of the liquid chemicals shifted towards lower frequencies as the dielectric constant of the chemical liquid increased. This is in agreement with the simulation results. A slight deviation was observed in the frequency resonance points in the measured results from the simulated results. A reason for this could be due to errors in the fabrication and measurement processes. Air gaps may exist in the FFF printed PLA substrate if the printer fails to print 100 percent infill of the substrate. This has the potential to affect the relative permittivity of the PLA substrate [25] and [26] and thus the results of any measurements including the frequency resonance point as well as the deviation Δf from the reference. The behavior of exhibited by Butanol-1-o1 and Propan-2-o1 in the simulation

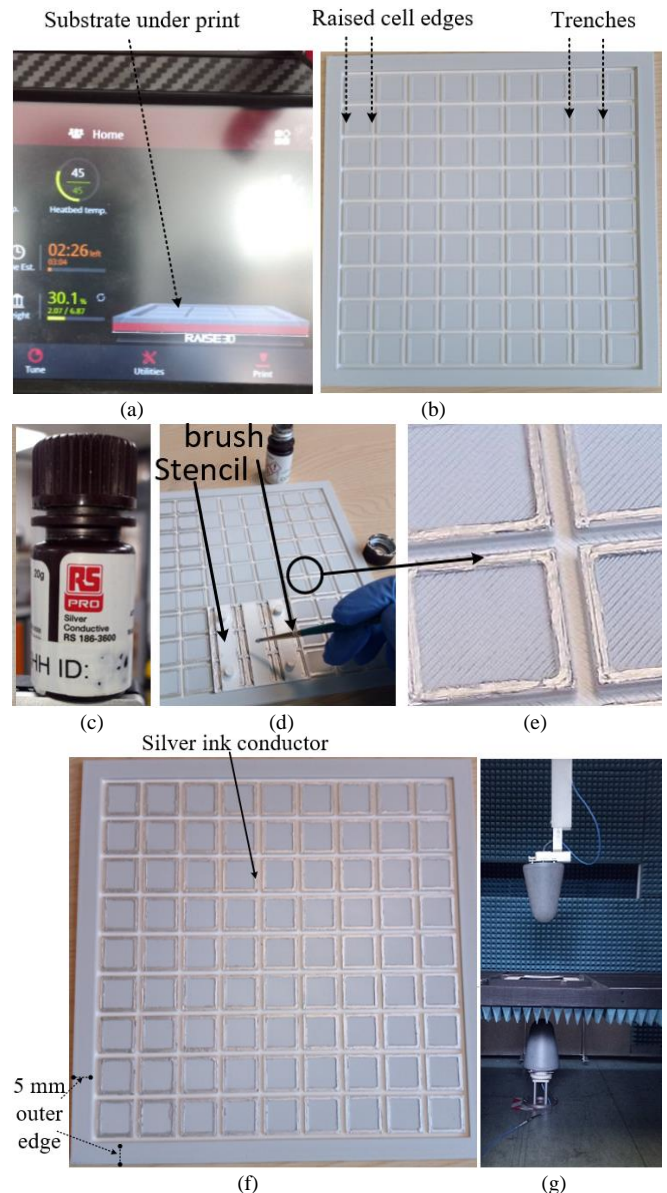


Fig. 4 The fabrication process of the 3D sensor (a) the printing of the substrate with a Raised 3D printer machine (b) the printed PLA substrate (c) the silver paint the printing of the substrate (d) applying silver loops (e) section of the painted FSS (f) the finished 3D FSS (g) the FSS sensor measurement setup.

results i.e., closeness of the results was replicated in the measurements.

IV. DISCUSSION AND CONCLUSION

A novel, inexpensive, 3D printed FSS sensor for sensing/detecting liquid chemicals has been demonstrated. The sensor has inter-element trenches where liquids can be deposited. Marked variations in resonance frequencies of the FSS have been observed when the trenches were filled with liquid chemicals of different electrical properties. The proposed microwave sensor has good sensitivity and low detection error.

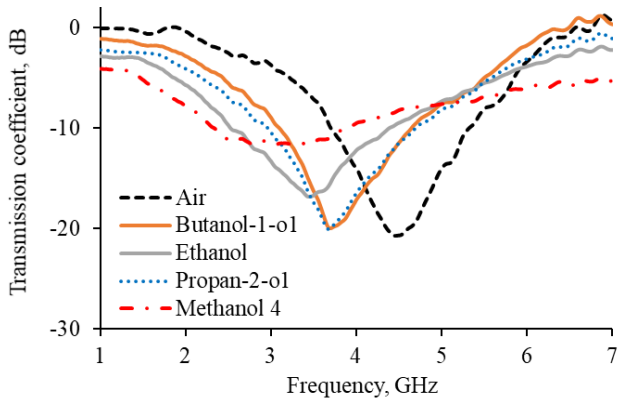


Fig. 5 The measured frequency response of the proposed sensor structure for the various liquid chemicals

TABLE IV
MEASURED RESONANCE FREQUENCY AND SHIFT FROM REFERENCE FREQUENCY

	Butanol-1-o1	Ethanol	Methanol	Propan-2-o1
f_s GHz	3.74	3.49	2.8	3.71
Δf GHz	0.69	0.94	1.89	0.72

The sensor is ideal for instances requiring real-time monitoring of liquids falling onto a surface. The contactless nature of the detection process would make it suitable for a critically safe working environment. Further, the FFF process used for the fabrication of the device has the advantage of reducing material cost, labour and manufacturing time. Its fabrication can also be quickly scaled up.

The structure of the sensor was found to twist and buckle after a few uses with the liquid chemical measured. This is likely to be due to the chemical interaction between the PLA substrate and the solvents employed [27]. This chemical interaction can also cause solvents to pass through the printed structure. This makes it a single use disposable detecting device. Other types of liquids such as water are unlikely to have the same effect on the PLA substrate, but this was not studied in this instance.

A future version of the design can be made for multiple use by printing with an inert material to prevent adverse chemical interaction between the substrate and the chemicals being tested.

ACKNOWLEDGMENT

The authors would like to thank Mr. A. Mendoza for his help with setting up the chamber and assisting in the measurement and Keith Greenhow who assisted in the fabrication of the FFF 3D printed sensor substrate. This work was part-funded by the EPSRC grant titled Low-Profile Ultra-Wideband WideScanning Multi-Function Beam-Steerable Array Antennas (EP/S005625/1) and the Royal Society Grant Ref: IEC\NSFC\191780 - International Exchanges 2019 Cost Share (NSFC).

REFERENCES

- [1] T. Scientific, "1-Butanol Safety Data Sheet," ThermoFisherScientific, Leicestershire, UK, 2020.
- [2] T. Scientific, "Ethanol, absolute Safety Data Sheet," ThermoFisher Scientific, Leicestershire, UK, 2020.
- [3] A. J. Cole and P. R. Young, "Chipless Liquid Sensing Using a Slotted Cylindrical Resonator," *IEEE SENSORS JOURNAL*, vol. 18, no. 1, pp. 149-156, 2018.
- [4] V. Makarovaite, A. J. R. Hillier, S. J. Holder, C. W. Gourlay and J. C. Batchelor, "Passive Wireless UHF RFID Antenna Label for Sensing Dielectric Properties of Aqueous and Organic Liquids," *IEEE SENSORS JOURNAL*, vol. 19, no. 11, pp. 4299-4307, 2019.
- [5] A. Ebrahimi, J. Scott and K. Ghorbani, "Microwave reflective biosensor for glucose level detection in aqueous solutions," *Sensors and Actuators A: Physical*, vol. 301, pp. 1-8, 2019.
- [6] Z. Geng, X. Zhang, Z. Fan, X. Lv and H. Chen, "A Route to Terahertz Metamaterial Biosensor Integrated with Microfluidics for Liver Cancer Biomarker Testing in Early Stage," *Scientific reports*, vol. 7, pp. 1-11, 2017.
- [7] A. A. M. Bahar, Z. Zakaria, M. K. M. Arshad, A. M. Isa, Y. Dasril and RammahA.Alahnomi, "Real Time Microwave Biochemical Sensor Based on Circular SIW Approach for Aqueous Dielectric Detection," *Scientific Reports*, vol. 9, pp. 1-12, 2019.
- [8] A. A. Abduljabar, D. J. Rowe, A. Porch and D. A. Barrow, "Novel Microwave Microfluidic Sensor Using a Microstrip Split-Ring Resonator," *IEEE TRANSACTIONS ON MICROWAVE THEORY AND TECHNIQUES*, vol. 62, no. 3, p. 679, 2014.
- [9] C.-S. Lee, B. Bai, Q.-R. Song, Z.-Q. Wang and G.-F. Li, "Open Complementary Split-Ring Resonator Sensor for Dropping-Based Liquid Dielectric Characterization," *IEEE SENSORS JOURNAL*, vol. 19, no. 24, pp. 11880-11890, 2019.
- [10] L. Su, J. Mata-Contreras, P. Vélaz, A. Fernández-Prieto and F. Martín, "Analytical Method to Estimate the Complex Permittivity of Oil Samples," *Sensors MPDI*, vol. 18, no. 4, pp. 1-12, 2018.
- [11] A. Salim and S. Lim, "Review of Recent Metamaterial Microfluidic Sensors," *MPDI Sensors*, vol. 18, no. 1, pp. 1-25, 2018.
- [12] E. L. Chuma, Y. Iano, G. Fontgalland and L. L. B. Roger, "Microwave Sensor for Liquid Dielectric Characterization Based on Metamaterial Complementary Split Ring Resonator," *IEEE SENSORS JOURNAL*, vol. 18, no. 24, pp. 9978-9983, 2018.
- [13] Z. Geng, X. Zhang, X. L. Zhiyuan Fan2 and H. Chen, "A Route to Terahertz Metamaterial Biosensor Integrated with Microfluidics for Liver Cancer Biomarker Testing in Early Stage," *Scientific Reports*, vol. 7, pp. 1-11, 2017.
- [14] A. Ebrahimi, W. Withayachumnankul, S. Al-Sarawi and D. Abbott, "High-Sensitivity Metamaterial-Inspired Sensor for Microfluidic Dielectric Characterization," *IEEE SENSORS JOURNAL*, vol. 14, no. 5, pp. 1345-1351, 2014.
- [15] S. Y. Jun, B. S. Izquierdo and E. A. Parker, "Liquid Sensor/Detector Using an EBG Structure," *IEEE TRANSACTIONS ON ANTENNAS AND PROPAGATION*, vol. 67, no. 5, pp. 3366-3373, 2019.
- [16] A. Arif, A. Zubair, K. Riaz, M. Q. Mehmood and M. Zubair, "A Novel Cesaro Fractal EBG-Based Sensing Platform for Dielectric Characterization of Liquids," *IEEE Transactions on Antennas and Propagation*, vol. 69, no. 5, pp. 2887 - 2895, 2021.
- [17] B. A. MUNK, *FREQUENCY SELECTIVE SURFACES: Theory and Design*, Chichester: JOHN WILEY & SONS, INC., 2000.
- [18] T. 3D, "FDM 3D printing – Fused Deposition," Tractus 3D, 01 10 2021. [Online]. Available: <https://tractus3d.com/knowledge/learn-3d-printing/fdm-3d-printing/>. [Accessed 01 10 2021].
- [19] R. J. LANGLEY and E. A. PARKER, "EQUIVALENT CIRCUIT MODEL FOR ARRAYS OF SQUARE LOOPS," *ELECTRONICS LETTERS*, vol. 18, no. 7, pp. 294-296, 1982.

- [20] A. Shastri, B. Sanz-Izquierdo, E. A. Parker, S. Gao, P. Reynaert and Z. Chen, "3D Printing of Millimetre Wave and Low-Terahertz Frequency Selective Surfaces Using Aerosol Jet Technology," *IEEE Access*, vol. 8, pp. 177341 - 177350, 2020.
- [21] S. Y. Jun, A. Elibiary, B. Sanz-Izquierdo, L. Winchester, D. Bird and A. McClelland, "3-D Printing of Conformal Antennas for Diversity Wrist Worn Applications," *IEEE TRANSACTIONS ON COMPONENTS, PACKAGING AND MANUFACTURING TECHNOLOGY*, vol. 8, no. 12, pp. 2227-2235, 2018.
- [22] A. P. Gregory and R. N. Clarke, "Tables of the Complex Permittivity of Dielectric Reference Liquids at Frequencies up to 5 GHz," National Physical Laboratory, Teddington, UK, 2012.
- [23] A. d. Lima, E. Parker and R. Langley, "Tunable frequency selective surface using liquid substrates," *Electronics Letters*, vol. 30, no. 4, pp. 281-282, 1994.
- [24] "RS PRO Liquid Conductive Paint," RS, 10 06 2021. [Online]. Available: <https://uk.rs-online.com/web/p/adhesives/1863600/>. [Accessed 10 06 2021].
- [25] P. F. Espin-Lopez, M. Pasian, G. Alaimo, S. Marconi, F. Auricchio, V. Heinänen and J. Järveläinen, "3-D Printed Antenna for Snowpack Monitoring," *IEEE Antennas and Wireless Propagation Letters*, vol. 17, no. 11, pp. 2109 - 2113, 2018.
- [26] B. Biernacki, S. Zhang and W. Whittow, "3D printed substrates with graded dielectric properties and their application to patch antennas," in *2016 Loughborough Antennas & Propagation Conference (LAPC)*, Loughborough, UK, 2016.
- [27] K. S. Erokhin, EvgeniyG.Gordeev and V. P. Ananikov, "Revealing interactions of layered polymeric materials at solid-liquid interface for building solvent compatibility charts for 3D printing applications," *Scientific Reports*, vol. 9, pp. 1-14, 2019.